Journal of Physics D:
Applied Physics

PAPER • **OPEN ACCESS**

High operating temperature (> 200 °C) InAs/GaAs quantum-dot laser with co-doping technique

To cite this article: Jae-Seong Park *et al* 2025 *J. Phys. D: Appl. Phys.* **58** 185101

OPEN ACCESS
IOP Publishing

Journal of Physics D: Applied Physics

J. Phys. D: Appl. Phys. **58** (2025) 185101 (8pp)

https://doi.org/10.1088/1361-6463/adc275

High operating temperature (> 200 °C) InAs/GaAs quantum-dot laser with co-doping technique

Jae-Seong Park[1,3], Huiwen Deng[1,3], Shujie Pan[1], Hexing Wang[1], Yangqian Wang[1], Jiajing Yuan[1], Xuanchang Zhang[1], Haotian Zeng[1], Hui Jia[1], Manyu Dang[1], Pawan Mishra[2], George Jandu[2], Siming Chen[1], Peter M Smowton[2], Alwyn Seeds[1], Huiyun Liu[1] and Mingchu Tang[1,*]

[1] Department of Electronic and Electrical Engineering, University College London, Torrington Place, London WC1E 7JE, United Kingdom
[2] School of Physics and Astronomy, Cardiff University, Cardiff CF10 3AT, United Kingdom

E-mail: Mingchu.tang@ucl.ac.uk

Received 13 December 2024, revised 7 March 2025
Accepted for publication 19 March 2025
Published 27 March 2025

Abstract

Working reliably at elevated operating temperatures is a key requirement for semiconductor lasers used in optical communication. InAs/GaAs quantum-dot (QD) lasers have been considered a promising solution due to the discrete energy states of QDs. This work demonstrates temperature-insensitive and low threshold InAs/GaAs QD lasers incorporating co-doping technique, compared with p-type modulation doping. 2 mm long co-doped QD lasers exhibit a low threshold current density of 154 A cm^{-2} (210 A cm^{-2}) and operate at a high heatsink temperature of 205 °C (160 °C) under the pulsed (continuous-wave) mode, outperforming the p-type doped QD lasers. The results reveal that co-doping effectively enhances both high-temperature stability and threshold reduction in InAs/GaAs QD lasers, surpassing the performance of conventional p-type modulation doping. This approach offers a pathway toward cooling-free operation, making co-doped QD lasers suitable for data and telecommunication applications.

Supplementary material for this article is available online

Keywords: semiconductor laser, quantum dot, molecular beam epitaxy

1. Introduction

Photonic integrated circuit (PIC)-based optical interconnects have become a more popular choice for data communication systems due to their advantages of high speed, large bandwidth, low power consumption and reduced latency [1–5]. However, robust light sources capable of operating in harsh environments with reduced cooling demand are crucial for commercialised optoelectronic applications, especially in data centres [6]. The need for a highly efficient and stable light-emitting source in data communication has brought the InAs/GaAs quantum-dot (QD) laser to the forefront [7]. The delta function-like density of states in QDs gives QD lasers superior optical and electrical properties, enabling them to exhibit temperature-insensitive operation, low threshold currents, and high tolerance to optical feedback [8–10]. InAs/GaAs QD lasers have also proven to

[3] These authors contributed equally to this work.
[*] Author to whom any correspondence should be addressed.

be excellent candidates as light sources for monolithic integration onto Si-based PICs, owing to their unique properties with high tolerance to crystal defects [11–14]. Furthermore, InAs/GaAs QDs have been demonstrated as an excellent active gain medium in multiple optical communication devices, including semiconductor optical amplifiers, comb lasers and photodetectors [15–18].

Despite the discrete energy states of QDs, the temperature-insensitive operation of QD lasers deviates from theoretical expectations, primarily due to the closed spaced valence band energy states. To enhance the performance of InAs/GaAs QD lasers at high temperatures, p-type modulation doping has been widely adopted, providing extra holes to the laser active region [19]. This technique has been shown to be effective in improving gain recovery, direct modulation response, ground-state quenching, and high-temperature stability [20–22]. However, it is commonly agreed that the p-type modulation doping in QD lasers can introduce extra free carrier absorption and non-radiative recombination, leading to a higher threshold current (I_{th}) [23]. For example, Kageyama *et al* reported that 8-stacked InAs/GaAs QD lasers (2 μm × 1200 μm) with p-type modulation doping achieved a record-high operating temperature of 220 °C, with a room-temperature (RT) threshold current density (J_{th}) of 625 A cm^{-2} [24]. On the other hand, n-type direct doping into the active region during the formation of QDs has been developed to reduce I_{th} and enhance the output power of QD lasers by passivating the non-radiative recombination centres and introducing extra electrons [25, 26]. However, it has been observed that in short cavity lengths, the high-temperature stability and tolerance to the ground-state quenching are relatively lower in n-doped QD lasers compared to p-type doped and undoped QD lasers [26]. Recently, the combination of n-type and p-type doping techniques, referred to as co-doping, has been found to enhance laser performance with respect to the I_{th}, maximum output power and high-temperature stability [27–29]. This co-doping strategy provides a low threshold and increased optical power due to the additional n-type direct doping while maintaining the high-temperature stability imparted by p-type doping. For instance, Lv *et al* demonstrated that co-doped QD lasers (6 μm × 1000 μm) under continuous-wave (CW) injection exhibited a lower RT J_{th} of 712 A cm^{-2}, compared to 1110 A cm^{-2} in p-doped QD lasers. Additionally, the co-doped QD lasers maintained a linear light–current (*L–I)* characteristic without saturation at 85 °C, whereas the p-doped QD lasers exhibited power saturation at 14 mW [27]. Deng *et al* also reported that the co-doped QD lasers exhibited high-temperature stability and effectively suppressed ground-state quenching, similar to p-type doped QD lasers [29], while achieving nearly half the J_{th} of p-type doped QD lasers.

In this paper, we demonstrate high-performance InAs/GaAs QD lasers with high operating temperature and low J_{th} by employing a co-doping technique, compared with p-type modulation doping. The fabricated narrow-ridge co-doped QD laser achieves a maximum operating temperature of 205 °C (160 °C) and a low J_{th} of 154 A cm^{-2} (210 A cm^{-2}) at RT under pulsed (CW) injection. In contrast, the p-type modulation doped QD laser presents slightly lower temperature stability and reduced output power. These results confirm that co-doping is a promising alternative to p-type modulation doping, effectively lowering J_{th} while maintaining high-temperature stability.

2. Material epitaxial growth and characterisation

The InAs/GaAs QD laser structure was grown on n-type GaAs (001) substrates, by using the Veeco GEN 930 molecular beam epitaxy (MBE) system. The epitaxial structure of QD lasers is shown in figure 1(a). To begin with the growth, the GaAs substrates were deoxidised in the MBE chamber under arsenic-rich conditions at 580 °C and followed by an initial 200 nm GaAs buffer layer to smooth the surface. The n-type cladding layer of a 1400 nm n-type $Al_{0.4}Ga_{0.6}As$ was grown, followed by 12 repeats of $Al_{0.4}Ga_{0.6}As$/GaAs superlattice layers (SPLs), each with a thickness of 1 nm, as a slab waveguide. The 7 layers of InAs dot-in-well (DWELL) structure, grown on a 2 nm $In_{0.16}Ga_{0.84}As$ quantum well and capped by a 4.5 nm $In_{0.16}Ga_{0.84}As$, were formed as an active region, with each DWELL layer separated by 43 nm of high-temperature-grown GaAs spacer layer [30]. To achieve the p-type modulation doping, 10 holes per dot (h/dot) were introduced in the GaAs spacer layer. For achieving the co-doping, an optimised doping density of 1.2 electrons per dot (e/dot) was implanted during the QD formation, with the p-type modulation doping. The laser structure was completed by 12 repeats of $Al_{0.4}Ga_{0.6}As$/GaAs SPLs as top slab waveguide, a 1400 nm p-type cladding layer, and a 300 nm heavily doped p-type GaAs contact layer.

The optical property of QDs has been examined by using photoluminescence (PL) measurements, using a 532 nm excitation laser, a Horiba 1000 M monochromator and a liquid nitrogen cooled InGaAs detector, as shown in figure 1(b). The full width at half maximum of the ground state peak reaches as low as 31.97 meV at RT with a peak wavelength of 1285 nm. To examine the QD morphology, an atomic force microscope (AFM) has been used to characterise the uncapped QDs. As presented in figures 1(c) and (d), the AFM images with a scan area of 1 × 1 μm^2 show a dot density of around 5.5 × 10^{10} cm^{-2} for both the modulation p-type doped and co-doped samples.

3. Laser fabrication and characteristic measurements

The InAs/GaAs QD lasers were fabricated into narrow-ridge-waveguide Fabry–Perot lasers with ridge widths of 8 μm. The ridges were formed using conventional photolithography and dry etching, followed by SiO_2 passivation. After opening the SiO_2 passivation layer within the ridge, a p-type metallisation layer of Ti/Pt/Au was deposited on the top of the ridge, and an additional Ti/Au layer was deposited as a bonding pad. The substrate was then thinned to 120 μm, and an n-type electrode of Ni/AuGe/Ni/Au was deposited on the backside of the substrate. To form Ohmic contacts, the samples were annealed

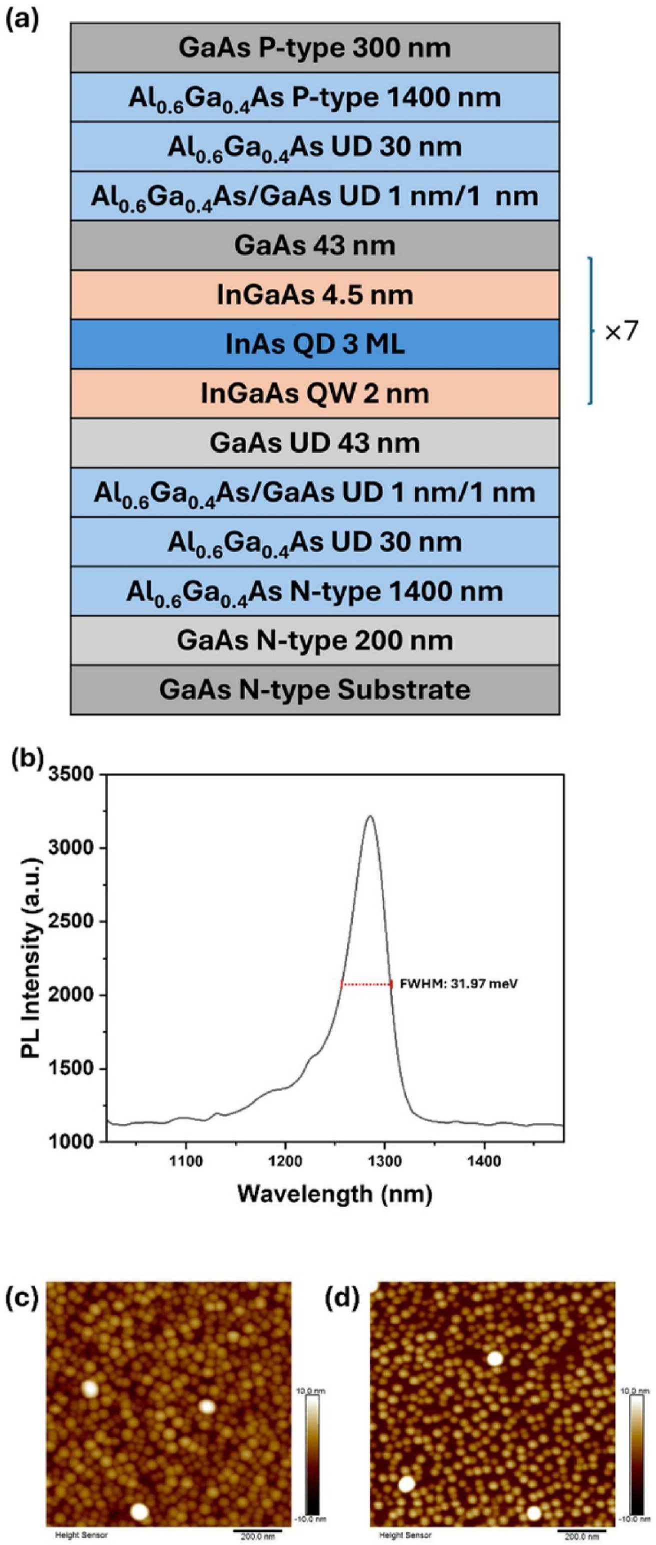

Figure 1. (a) Epitaxial structure of InAs/GaAs QD laser. (b) Room temperature PL spectrum of InAs/GaAs QDs. A representative AFM image of a (c) p-type modulation doped and (d) co-doped uncapped QD sample.

at 410 °C for 1 min. Laser bars were cleaved into 2 mm cavity lengths. High reflectivity coatings of 50% and 90% reflectivity were applied to the front and rear facets, respectively. The laser devices were flip-bonded onto the AlN submount using AuSn solder and Au wire bonding. To measure the performance of the QD lasers at different temperatures, the devices were mounted on a copper heatsink/thermoelectric cooling module equipped with a resistance thermometer. The temperature was controlled by an LDT-5948 unit, utilising four-wire voltage and sensor measurements.

Figures 2(a) and (b) show the CW temperature-dependent *L–I* measurement for the co-doped and p-type doped InAs/GaAs QD lasers with 8 μm × 2000 μm ridges, respectively. For the co-doped QD laser, the I_{th} at RT was 33.7 mA, corresponding to the J_{th} of 210 A cm^{-2}, while the p-type doped QD laser obtained the I_{th} of 38.4 mA, corresponding to the J_{th} of 240 A cm^{-2}. It is evident that both co-doped and p-type doped QD lasers operate successfully up to 160 °C. To better illustrate the subtle variations of *L–I* characteristics as a function of temperature, the *L–I* curves with a reduced power scale are also presented in the supplementary information (figure S1). Figure 2(c) summarises the J_{th} trend for the co-doped and p-type doped QD lasers over the temperature range of 20 °C–160 °C. Overall, the co-doped QD laser exhibits lower J_{th} values compared to the p-type doped QD laser, which can be attributed to the additional electron doping in the co-doped active region. Based on the temperature dependence of J_{th}, the characteristic temperature (T_0) of the devices was calculated for the different temperature ranges (20 °C–80 °C and 80 °C–120 °C). For the co-doped QD laser, T_0 values were measured to be 217.4 K for 20 °C–80 °C and 104.3 K for 80 °C–120 °C, while the p-type doped QD laser exhibited T_0 values of 332.2 K for 20 °C–80 °C and 116.7 K for 80 °C–120 °C. The higher T_0 values of the p-type doped QD laser up to 120 °C indicate its relatively better thermal stability compared to the co-doped QD laser. However, at temperatures above 120 °C, the co-doped sample demonstrates performance similar to that of the p-doped QD laser.

Figures 3(a) and (b) present the lasing spectra for the co-doped and p-type doped QD lasers at various temperatures, measured at an injection current of 1.1 × I_{th}. The peak lasing wavelengths for the co-doped and p-type doped InAs/GaAs QD lasers red-shifted from 1305 nm to 1368 nm and from 1294 nm to 1360 nm, respectively, as the temperature increased from 20 °C to 160 °C, and the temperature-induced wavelength shifts were measured to be 0.46 nm °C^{-1} and 0.47 nm °C^{-1}, respectively. It is evident that for both QD lasers, ground-state lasing is consistently observed up to 160 °C. Note that the RT peak lasing wavelength of the co-doped QD laser is red-shifted compared to the p-type doped QD laser, likely due to the valence band shift caused by injecting extra electrons [21].

To reduce the impact of the self-heating effect on the temperature characteristics, the fabricated InAs/GaAs QD lasers were also tested under pulsed mode (1 μs pulse width and 1% duty cycle). Figure 4(a) shows the co-doped QD laser operating at a maximum temperature of 205 °C, which is slightly higher than the 200 °C observed for the p-type doped QD laser (figure 4(b)). The I_{th} at RT for the co-doped and p-type doped QD lasers was 24.7 and 25.8 mA, corresponding to the J_{th} of 154 and 161 A cm^{-2}, respectively. For improved clarity in the

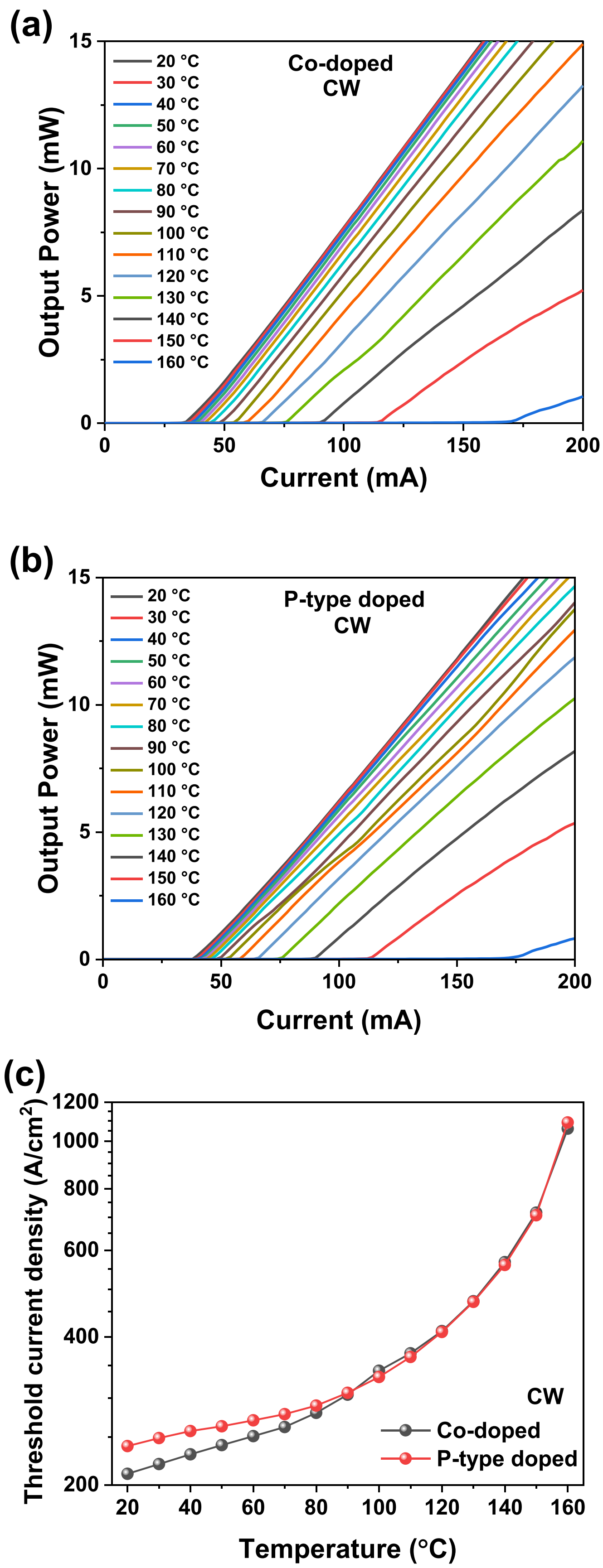

Figure 2. Temperature-dependent *L–I* curves of (a) co-doped and (b) p-type doped InAs/GaAs QD lasers under CW operation. (c) J_{th} versus temperature trend for the co-doped and p-type doped InAs/GaAs QD lasers under CW operation.

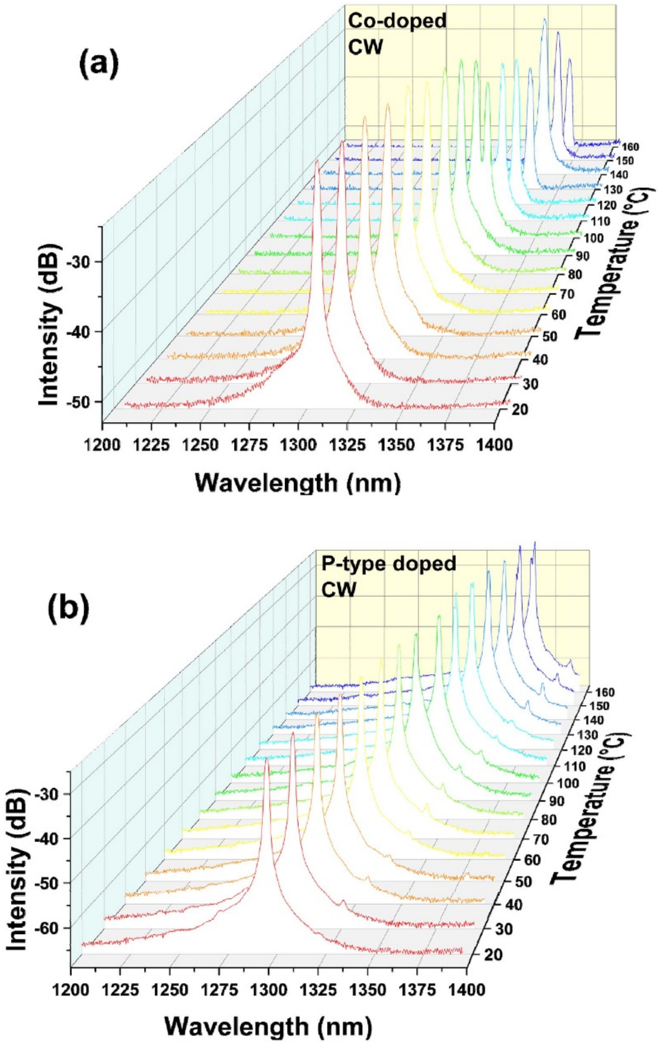

Figure 3. Lasing spectra for (a) co-doped and (b) p-type doped QD lasers over the temperature range of 20 °C–160 °C under CW operation.

overlapped region of the temperature-dependent *L*–*I* curves, plots with a reduced power scale are also provided in the supplementary information (figure S2). The J_{th} trend is presented in figure 4(c). Both QD lasers produce similar J_{th} values up to 180 °C, but the co-doped QD laser achieves lower J_{th} values in the higher temperature range of 180 °C–200 °C. The co-doped QD laser presents T_0 values of 840.3 K for 20 °C–80 °C and 129.0 K for 80 °C–120 °C, while the p-type doped QD laser exhibits T_0 values of 617.3 K for 20 °C–80 °C and 180.5 K for 80 °C–120 °C.

The lasing spectra of the co-doped and p-type doped QD lasers under pulsed injection were also measured across various temperatures at an injection current of 1.1 × I_{th}, as shown in figures 5(a) and (b), respectively. For both QD lasers, ground-state lasing was achieved up to 170 °C, while excited-state lasing was observed at 180 °C and above. The peak lasing wavelengths at RT were 1305 nm for the co-doped QD lasers and 1294 nm for the p-type doped QD lasers, and the wavelength shifts for ground-state lasing were measured to be 0.44 nm $°C^{-1}$ and 0.46 nm $°C^{-1}$, respectively.

To further evaluate the output power of the InAs/GaAs QD lasers with co-doping and p-type modulation doping techniques, the injection current was increased to 0.8 A under CW mode and to 1 A under pulsed mode at RT. Figure 6(a) shows the light–current–voltage (*LIV*) curves for CW mode. The co-doped QD laser achieved a maximum power of 80 mW at an injection current of 0.8 A, with a slope efficiency of 0.134 W A^{-1}. In comparison, the p-type doped QD laser produced a maximum power of 78 mW and a slope efficiency of 0.120 W A^{-1}. As shown in figure 6(b), under the pulsed mode, the co-doped and p-type doped QD lasers exhibited maximum powers of 133 mW and 122 mW at an injection current of 1 A, with slope efficiencies of 0.134 W A^{-1} and 0.126 W A^{-1}, respectively.

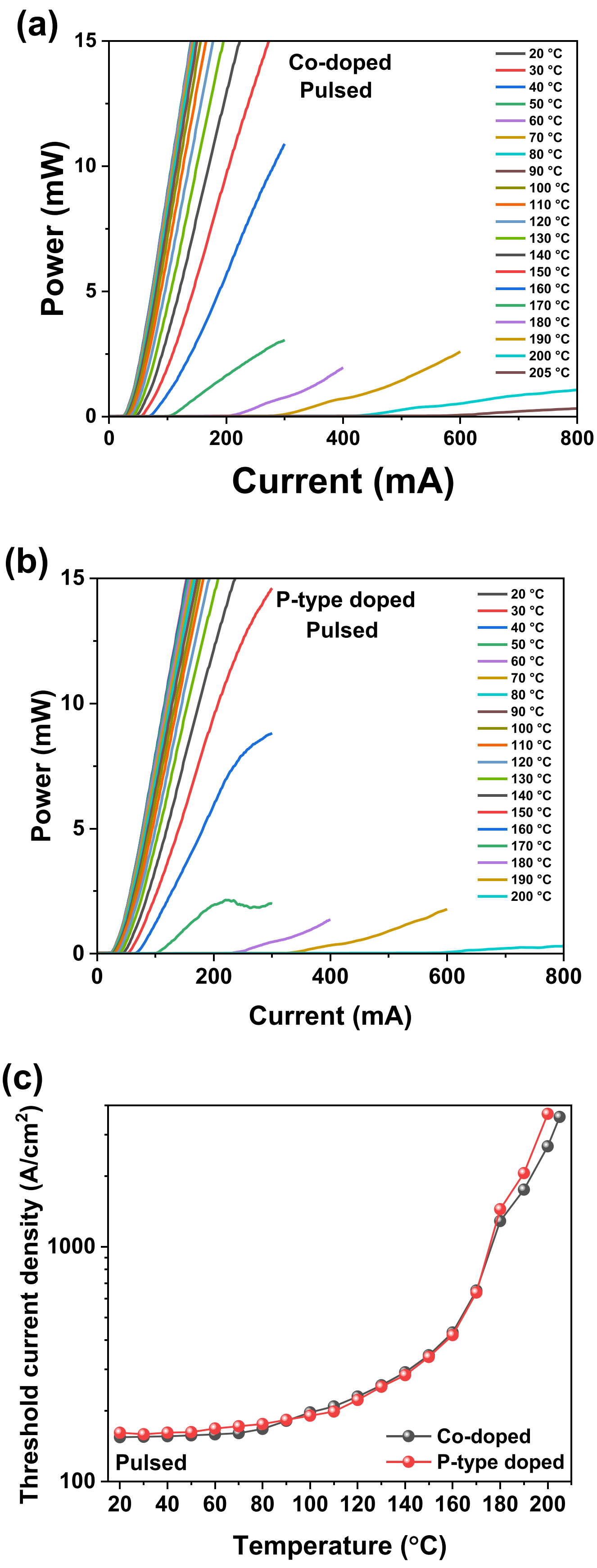

Figure 4. Temperature-dependent *L–I* measurements of (a) co-doped and (b) p-type doped InAs/GaAs QD lasers under pulsed mode. (c) The J_{th} versus temperature trend of the co-doped and p-type doped InAs/GaAs QD lasers under pulsed mode.

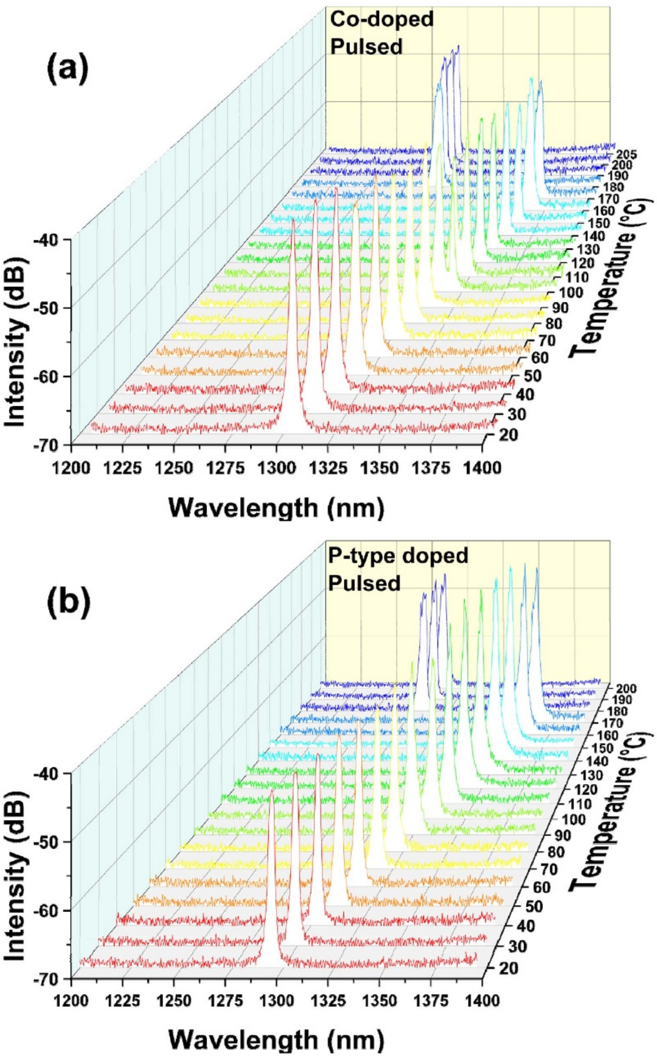

Figure 5. Lasing spectra for (a) co-doped and (b) p-type doped QD lasers over a temperature range of 20 °C–205 °C under pulsed mode.

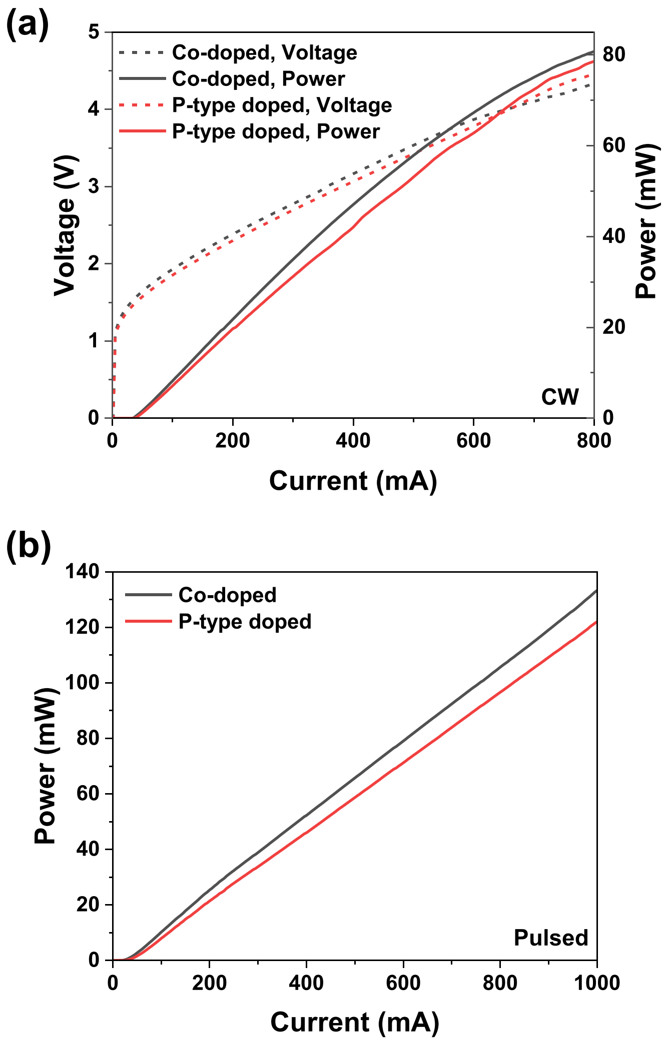

Figure 6. (a) The *LIV* curves for the narrow-ridge lasers under CW modes. (b) The *LI* curves for the narrow-ridge lasers under pulse mode.

4. Discussion and conclusion

High-performance InAs/GaAs QD lasers capable of operating at extremely high temperatures were attained. A comparative analysis of 7-layer QD lasers with co-doping and p-type modulation doping revealed the superior performance of co-doped QD lasers in terms of J_{th}, output power, and temperature stability. Specifically, the co-doped QD lasers demonstrated maximum operating temperatures of 160 °C (205 °C) under CW (pulsed) injection, which is slightly better than the 160 °C (200 °C) observed for the p-type doped QD lasers. Additionally, the co-doped QD lasers achieved a J_{th} of 210 A cm^{-2} under CW mode (154 A cm^{-2} under pulsed mode) and a slope efficiency of 0.134 W A^{-1} in both modes at RT, outperforming the p-type doped QD lasers. This work demonstrates significant progress in enhancing the temperature-insensitive performance of InAs/GaAs QD lasers with a low J_{th} by employing co-doping. The results highlight the effectiveness of the co-doping strategy in leveraging the high-temperature stability of p-type modulation doping while benefiting from the low threshold of direct n-type doping, thereby mitigating the typical drawbacks of each method. As a result, the co-doping technique emerges as a viable alternative to p-type modulation doping for achieving both high-temperature stability and low J_{th} in InAs/GaAs QD lasers. Furthermore, the co-doped InAs/GaAs QD lasers demonstrated in this study show great potential as a promising light source for cooling-free environments in optical communication applications.

Data availability statement

All data that support the findings of this study are included within the article (and any supplementary files).

Acknowledgments

This work was supported by the UK Engineering and Physical Sciences Research Council (EP/Z532848/1, EP/P006973/1,

EP/R029075/1, EP/T028475/1, EP/V029606/1, and EP/X015300/1), and European Union's Horizon 2020 programme under grant agreement number 101129904.

ORCID iDs

Jae-Seong Park https://orcid.org/0000-0002-6486-2342
Xuanchang Zhang https://orcid.org/0009-0007-0382-2981
Hui Jia https://orcid.org/0000-0002-8325-3948
George Jandu https://orcid.org/0009-0006-0758-9817
Siming Chen https://orcid.org/0000-0002-4361-0664
Peter M Smowton https://orcid.org/0000-0002-9105-4842
Huiyun Liu https://orcid.org/0000-0002-7654-8553
Mingchu Tang https://orcid.org/0000-0001-6626-3389

References

[1] Kash J A, Benner A F, Doany F E, Kuchta D M, Lee B G, Pepeljugoski P K, Schares L, Schow C L and Taubenblatt M 2011 Optical interconnects in future servers *2011 Optical Fiber Communication Conf. and Exposition and the National Fiber Optic Engineers Conf.* pp 1–3
[2] Heck M J R and Bowers J E 2014 Energy efficient and energy proportional optical interconnects for multi-core processors: driving the need for on-chip sources *IEEE J. Sel. Top. Quantum Electron.* **20** 332–43
[3] Haurylau M, Chen G, Chen H, Zhang J, Nelson N A, Albonesi D H, Friedman E G and Fauchet P M 2006 On-chip optical interconnect roadmap: challenges and critical directions *IEEE J. Sel. Top. Quantum Electron.* **12** 1699–705
[4] Shi Y, Zhang Y, Wan Y, Yu Y, Zhang Y, Hu X, Xiao X, Xu H, Zhang L and Pan B 2022 Silicon photonics for high-capacity data communications *Photon. Res.* **10** A106–34
[5] Thomson D *et al* 2016 Roadmap on silicon photonics *J. Opt.* **18** 073003
[6] Cheng Q, Bahadori M, Glick M, Rumley S and Bergman K 2018 Recent advances in optical technologies for data centers: a review *Optica* **5** 1354–70
[7] Nishi K, Takemasa K, Sugawara M and Arakawa Y 2017 Development of quantum dot lasers for data-com and silicon photonics applications *IEEE J. Sel. Top. Quantum Electron.* **23** 1–7
[8] Arakawa Y and Sakaki H 1982 Multidimensional quantum well laser and temperature dependence of its threshold current *Appl. Phys. Lett.* **40** 939–41
[9] Huang H, Duan J, Jung D, Liu A Y, Zhang Z, Norman J, Bowers J E and Grillot F 2018 Analysis of the optical feedback dynamics in InAs/GaAs quantum dot lasers directly grown on silicon *J. Opt. Soc. Am.* B **35** 2780–7
[10] Duan J, Huang H, Jung D, Zhang Z, Norman J, Bowers J E and Grillot F 2018 Semiconductor quantum dot lasers epitaxially grown on silicon with low linewidth enhancement factor *Appl. Phys. Lett.* **112** 251111
[11] Chen S *et al* 2016 Electrically pumped continuous-wave III–V quantum dot lasers on silicon *Nat. Photon.* **10** 307–11
[12] Wei W-Q *et al* 2023 Monolithic integration of embedded III–V lasers on SOI *Light Sci. Appl.* **12** 84
[13] Tang M, Park J-S, Wang Z, Chen S, Jurczak P, Seeds A and Liu H 2019 Integration of III–V lasers on Si for Si photonics *Prog. Quantum Electron.* **66** 1–18
[14] Shang C *et al* 2022 Electrically pumped quantum-dot lasers grown on 300 mm patterned Si photonic wafers *Light Sci. Appl.* **11** 299
[15] Dong B, Dumont M, Terra O, Wang H, Netherton A and Bowers J E 2023 Broadband quantum-dot frequency-modulated comb laser *Light Sci. Appl.* **12** 182
[16] Liu S, Wu X, Jung D, Norman J C, Kennedy M J, Tsang H K, Gossard A C and Bowers J E 2019 High-channel-count 20 GHz passively mode-locked quantum dot laser directly grown on Si with 4.1 Tbit/s transmission capacity *Optica* **6** 128–34
[17] Krishna S 2005 Quantum dots-in-a-well infrared photodetectors *J. Phys. D: Appl. Phys.* **38** 2142
[18] Sogabe T, Shen Q and Yamaguchi K 2016 Recent progress on quantum dot solar cells: a review *J. Photonics Energy* **6** 040901
[19] Deppe D G, Huang H and Shchekin O B 2002 Modulation characteristics of quantum-dot lasers: the influence of p-type doping and the electronic density of states on obtaining high speed *IEEE J. Quantum Electron.* **38** 1587–93
[20] Shchekin O B and Deppe D G 2002 The role of p-type doping and the density of states on the modulation response of quantum dot lasers *Appl. Phys. Lett.* **80** 2758–60
[21] Maximov M V, Shernyakov Y M, Zubov F I, Zhukov A E, Gordeev N Y, Korenev V V, Savelyev A V and Livshits D A 2013 The influence of p-doping on two-state lasing in InAs/InGaAs quantum dot lasers *Semicond. Sci. Technol.* **28** 105016
[22] Zhang Z, Jung D, Norman J C, Patel P, Chow W W and Bowers J E 2018 Effects of modulation p doping in InAs quantum dot lasers on silicon *Appl. Phys. Lett.* **113** 061105
[23] Norman J C, Zhang Z, Jung D, Shang C, Kennedy M J, Dumont M, Herrick R W, Gossard A C and Bowers J E 2019 The importance of p-doping for quantum dot laser on silicon performance *IEEE J. Quantum Electron.* **55** 1–11
[24] Kageyama T, Nishi K, Yamaguchi M, Mochida R, Maeda Y, Takemasa K, Tanaka Y, Yamamoto T, Sugawara M and Arakawa Y 2011 Extremely high temperature (220 °C) continuous-wave operation of 1300-nm-range quantum-dot lasers *2011 Conf. on Lasers and Electro-Optics Europe and 12th European Quantum Electronics Conf.* p 1
[25] Lv Z-R, Zhang Z-K, Yang X-G and Yang T 2018 Improved performance of 1.3-μm InAs/GaAs quantum dot lasers by direct Si doping *Appl. Phys. Lett.* **113** 011105
[26] Deng H *et al* 2022 The role of different types of dopants in 1.3 μm InAs/GaAs quantum-dot lasers *J. Phys. D: Appl. Phys.* **55** 215105
[27] Lv Z-R, Wang S, Wang H, Wang H-M, Chai H-Y, Yang X-G, Meng L, Ji C and Yang T 2022 Significantly improved performances of 1.3 μm InAs/GaAs QD laser by spatially separated dual-doping *Appl. Phys. Lett.* **121** 021105
[28] Wang S, Lv Z, Wang S, Chai H, Meng L, Yang X and Yang T 2023 Significantly enhanced performance of InAs/GaAs quantum dot lasers on Si(001) via spatially separated co-doping *Opt. Express* **31** 20449–56
[29] Deng H *et al* 2024 1.3 μm InAs/GaAs quantum-dot lasers with p-type, n-type, and co-doped modulation *Adv. Phys. Res.* **3** 2400045
[30] Liu H Y, Hopkinson M, Harrison C N, Steer M J, Frith R, Sellers I R, Mowbray D J and Skolnick M S 2003 Optimizing the growth of 1.3 μm InAs/InGaAs dots-in-a-well structure *J. Appl. Phys.* **93** 2931–6